

## Supporting Information

### Selective Separation of Single-Walled Carbon Nanotubes in Aqueous Solution by Assembling Redox Nanoclusters

Anquan Zhu<sup>#</sup>, Xusheng Yang<sup>#</sup>, Lei Zhang, Kun Wang, Tianhui Liu, Xin Zhao, Luyao Zhang, Lei Wang, Feng Yang\*

#### Experiment Section

**Preparation of Cluster-SWCNT Hybrids.** Tuball-SWCNTs (purity>90%,  $d_t=0.9-2.2$  nm) were provided from the OCSiAl company. CoMo-SWCNTs were purchased from Sigma Aldrich (CG100, purity>89%,  $d_t=0.7-1.3$  nm).  $H_3PW_{12}O_{40}\cdot xH_2O$  was purchased from Meryer (Shanghai) Chemical Technology Co., Ltd.  $Na_2WO_4\cdot 2H_2O$  was bought from Shanghai Aladdin Biochemical Technology Co., Ltd.  $H_6P_2W_{18}O_{62}\cdot xH_2O$  and  $K_{12}H_2P_2W_{12}O_{48}\cdot xH_2O$  were synthesized according to the reported methods. For a typical process of synthesizing the  $\{PW_{12}O_{40}\}@Tuball-SWCNTs$ , the raw SWCNTs were annealed in air at 420 °C for 5 min to open ends of nanotubes. For the synthesis of  $\{PW_{12}O_{40}\}-CoMo-SWCNTs$ , annealing process is not necessary. Then, the SWCNTs (40 mg) were mixed with aqueous  $\{PW_{12}O_{40}\}$  solution (800 mg  $\{PW_{12}O_{40}\}/12$  mL deionized water). The mixture was stirred for 4 days at room temperature. Then the  $\{PW_{12}O_{40}\}@SWCNTs$  were isolated by centrifugation and washed with deionized water for 10 times to remove  $\{PW_{12}O_{40}\}$  clusters outside nanotubes. After drying at room temperature, the  $\{PW_{12}O_{40}\}@SWCNT$  hybrids were collected. Other types of clusters and salts ( $H_6P_2W_{18}O_{62}\cdot xH_2O$ ,  $K_{12}H_2P_2W_{12}O_{48}\cdot xH_2O$ , and  $Na_2WO_4\cdot 2H_2O$ ) within SWCNTs were carried out by the same method.

**Dispersion of SWCNTs in DOC Aqueous Solution.** DOC ( $C_{24}H_{39}O_4Na$ , 98%) was purchased from Shanghai Aladdin Biochemical Technology Co., Ltd, and used to

disperse SWCNTs. Typically, 2 mg {PW<sub>12</sub>O<sub>40</sub>}@SWCNT hybrids were added into 20 mL 1 wt% DOC solution, followed with a sonication treatment by using a tip ultrasonicator (500 W in pulse mode with 2 s on/3 s off interval) for 80 min. After that, the resulting suspension was centrifuged at 13000 g for 1 h to remove the precipitation of SWCNT bundles. Then the supernatant was collected for measurement. The pristine SWCNTs and other cluster@SWCNT hybrids were dispersed by 1 wt% DOC aqueous solution with the same method.

***SEM and TEM Characterization.*** SEM images were recorded on a ZEISS Merlin SEM operating at 1.0 kV. HAADF-STEM images were collected from a FEI Titan I Titan Themis apparatus with an X-FEG electron gun and a DCOR aberration corrector operating at 300 kV. STEM-EDX mapping was performed on an FEI Talos F200X electron microscope with a HAADF detector and acceleration voltage of 200 kV. EDX was acquired from a Bruker super-X detection system.

***Characterization of SWCNTs.*** UV-Vis-NIR absorption spectra were measured by using a Shimadzu UV-2600 spectrometer. The Raman spectra of the SWCNT and cluster@SWCNT aqueous dispersions were collected with a Jovin Yvon-Horiba LabRam HR evolution system (laser excitations: 532 and 785 nm). In addition, the SWCNT and {PW<sub>12</sub>O<sub>40</sub>}@SWCNT dispersion were deposited on Si/SiO<sub>2</sub> substrate to obtain individual nanotubes for Raman and AFM (Veeco diMutiMode V, operated at tapping mode) measurements.

## RESULTS

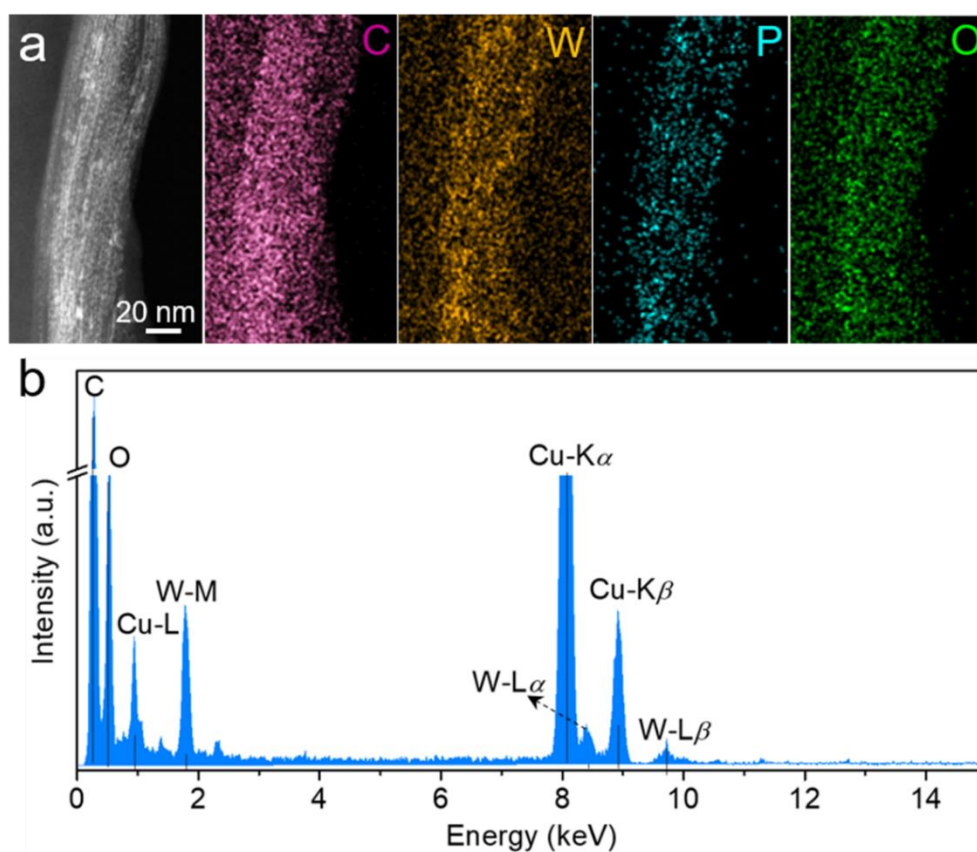


**Figure S1.** **a**, HAADF-STEM image of  $\{PW_{12}O_{40}\}@Tuball-SWCNTs$  and STEM-EDX elemental mapping. **b**, EDX spectrum.

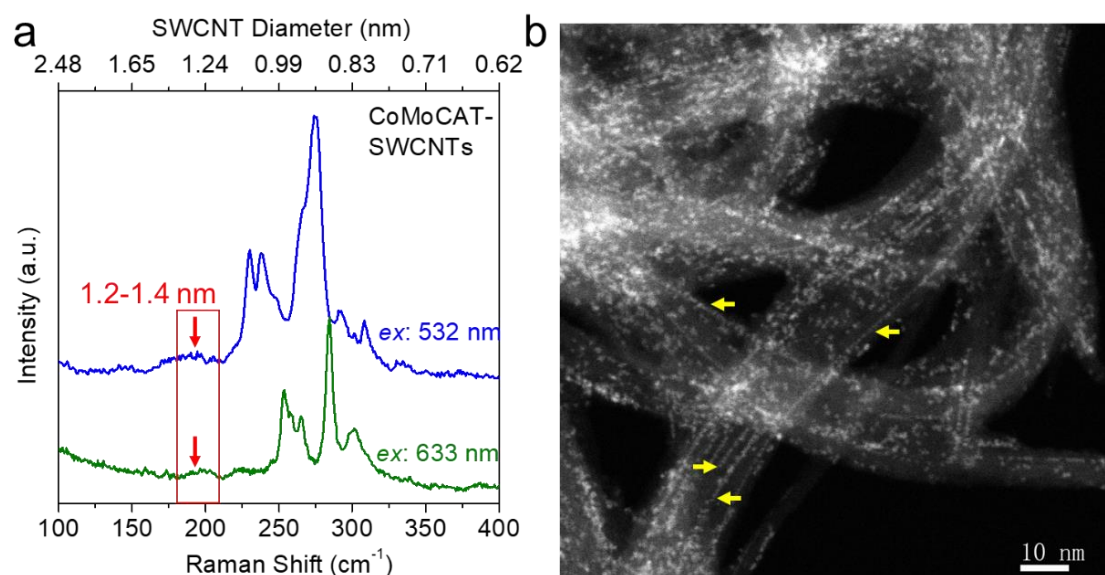


**Figure S2. a**, Raman spectra of pristine CoMo-SWCNTs (excitation wavelength: 532 nm and 633 nm). **b**, HAADF-STEM images of CoMo-SWCNTs with  $\{PW_{12}O_{40}\}$ . The cluster encapsulated within SWCNT as a linear structure was marked by arrows.

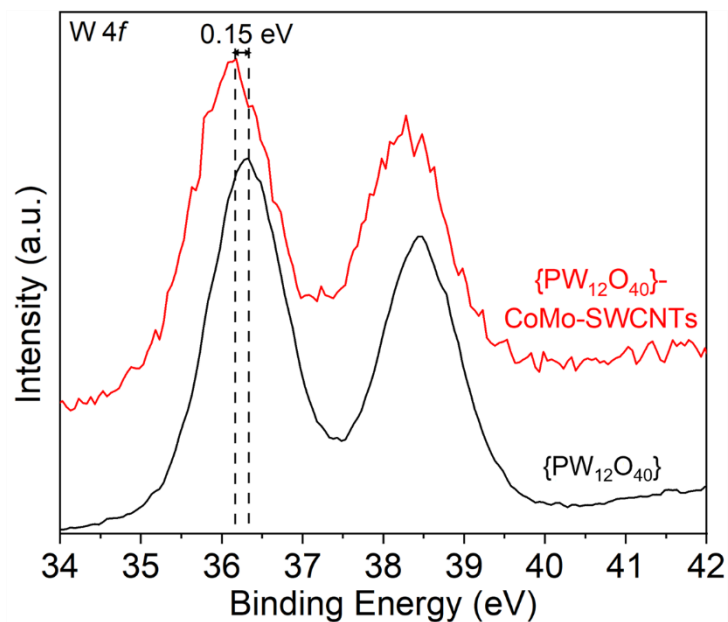


**Figure S3.** The XPS W 4f spectra of  $\{PW_{12}O_{40}\}$  and  $\{PW_{12}O_{40}\}$ -CoMo-SWCNT hybrid.

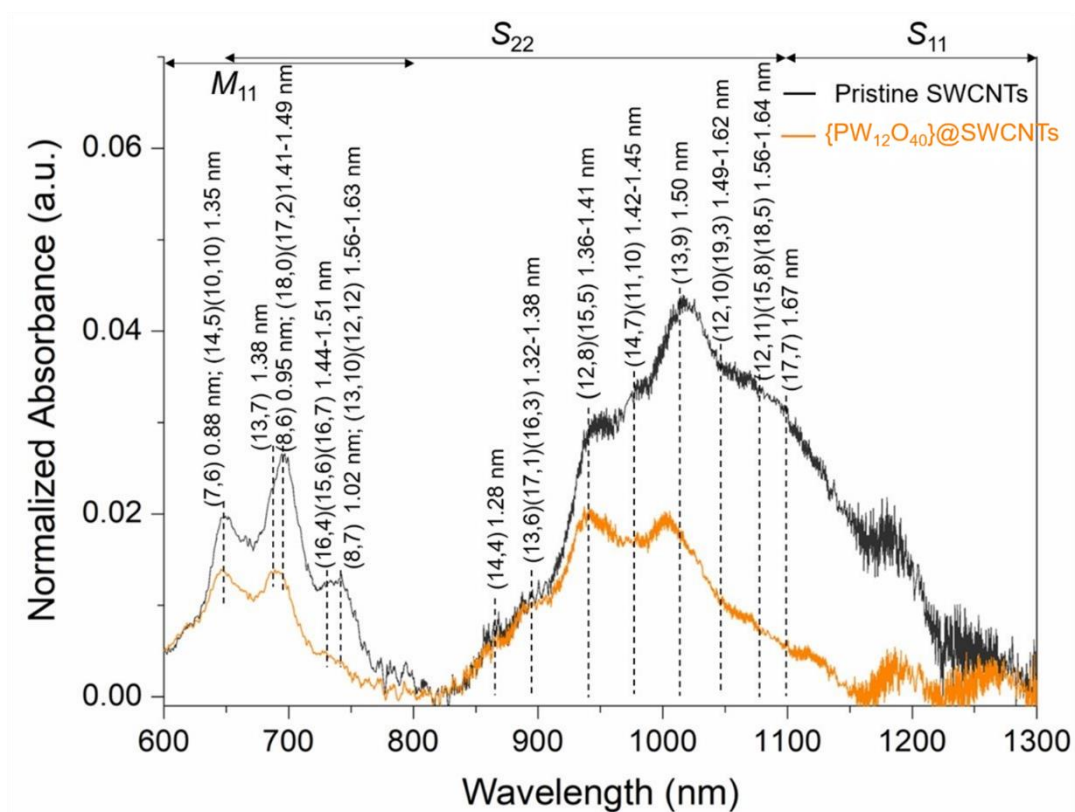


**Figure S4.** The possible chirality assignment of DOC-dispersed Tuball-SWCNTs.

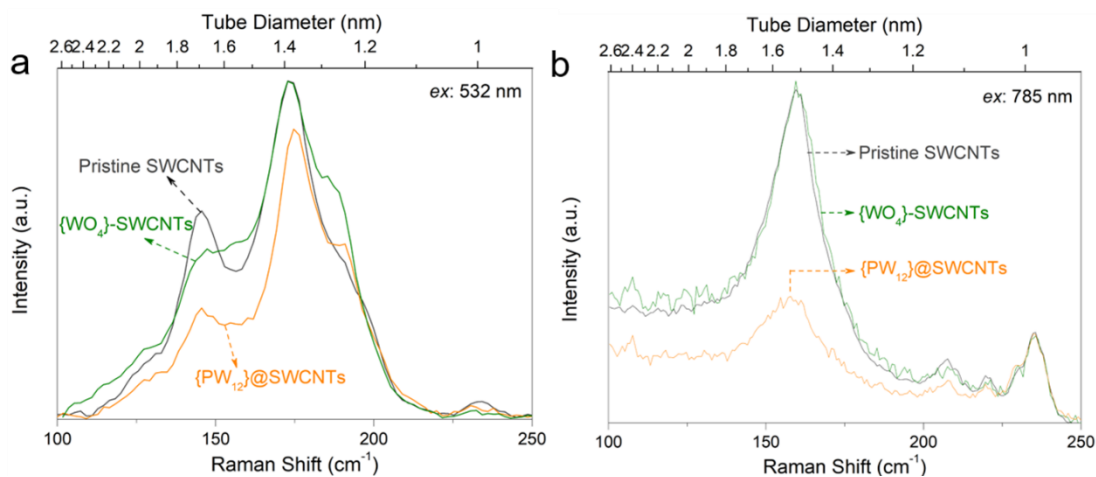


**Figure S5. a, b,** Raman spectra of the dispersed pristine Tuball-SWCNTs and cluster@Tuball-SWCNTs showing RBM region ( $\omega_{RBM}=214.4/d_t+18.7$ ). Laser excitations: 532 nm (a), 785 nm (b). The pristine Tuball-SWCNTs were used as a reference. RBM region was normalized relative to the intensity of the smallest tube diameter, with RBM frequency at  $230\text{ cm}^{-1}$ .

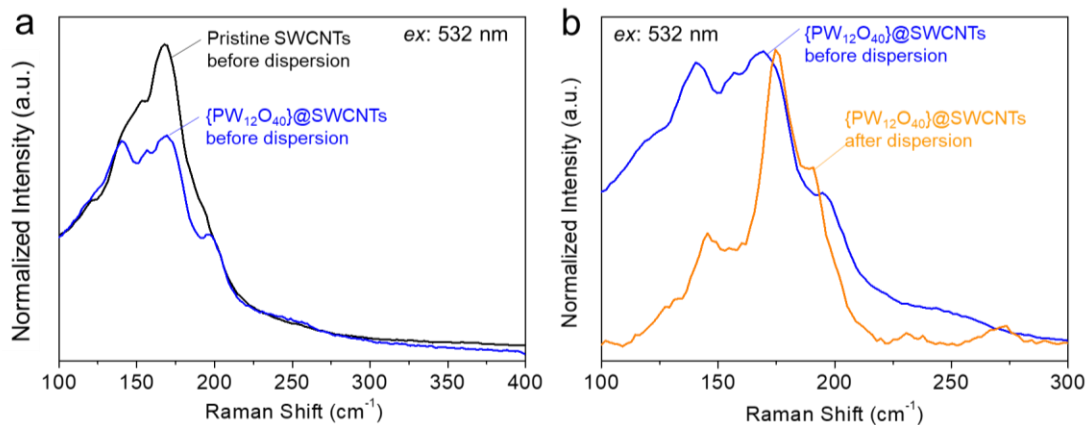


**Figure S6.** **a**, Raman RBM region of pristine and  $\{PW_{12}O_{40}\}$  encapsulated Tuball-SWCNT powder samples before dispersion. **b**, Raman RBM region of  $\{PW_{12}O_{40}\}$ @SWCNTs before and after dispersion. The spectra were calibrated with respect to Si peak ( $302.5\text{ cm}^{-1}$ ).

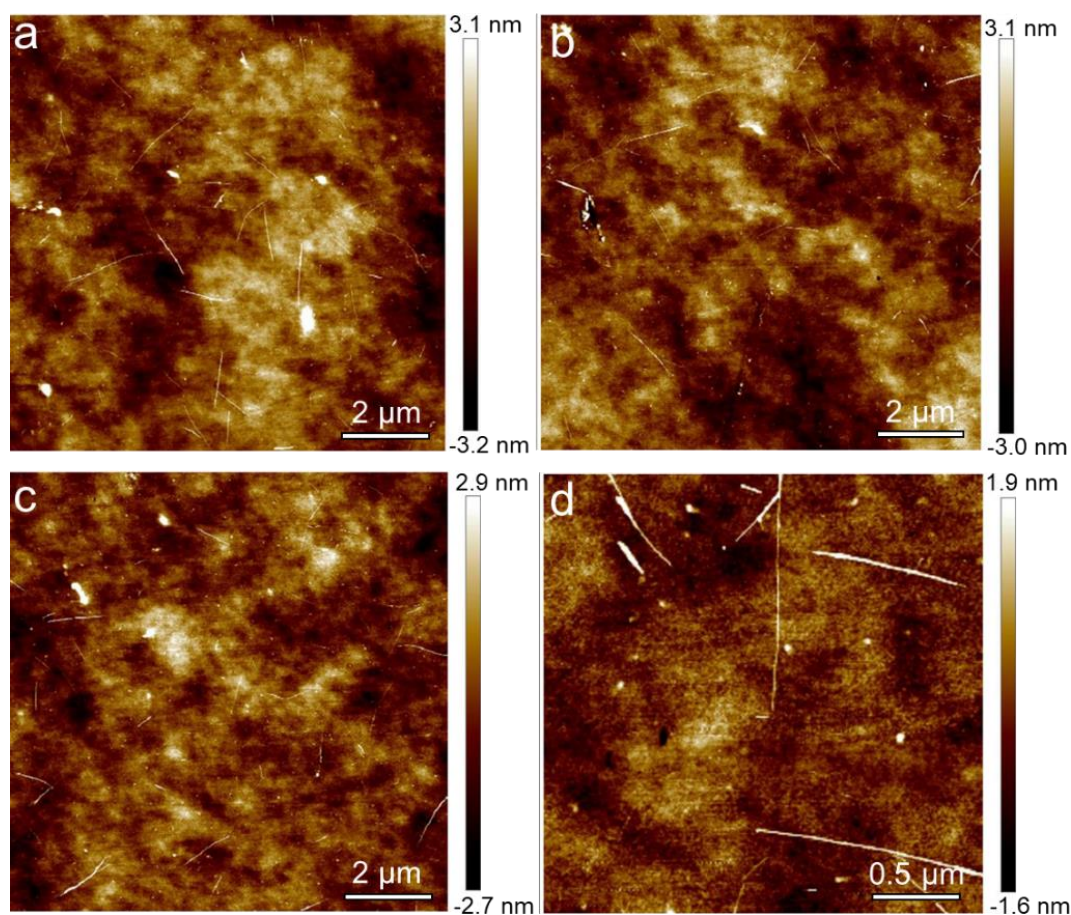


**Figure S7.** **a–d**, Atomic force microscopy images of dispersed  $\{PW_{12}O_{40}\}$ @Tuball-SWCNTs.



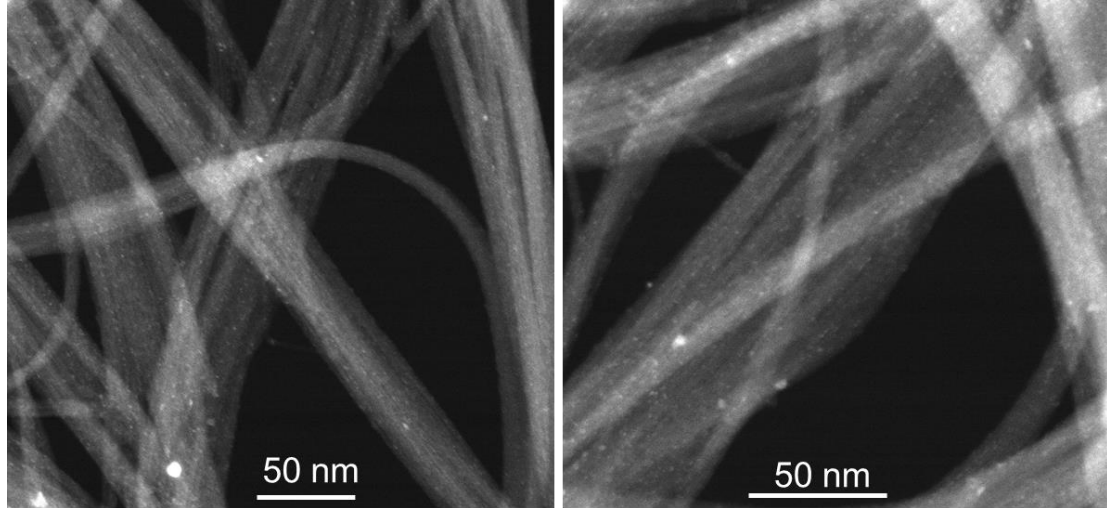


**Figure S8.** Typical HAADF-STEM images of  $\text{WO}_4^{2-}$ -Tuball-SWCNTs.

The smallest SWCNTs ( $d_{\text{tube}}$ ) encapsulating a  $\{\text{PW}_{12}\}$  cluster can be estimated by the following model (Fig. S9), where ionic bonding between  $\text{O}^{2-}$  of  $\{\text{PW}_{12}\}$  and C cation of graphene lattice is considered.

$$y \approx \text{ionic radius of } \text{O}^{2-} + \text{ionic radius of } \text{C}^+ = 1.26 \text{ \AA} + 0.95 \text{ \AA} = 2.21 \text{ \AA}$$

where ionic radius of  $\text{C}^+$  (0.95 Å) is estimated based on the tropylium cation ( $\text{C}_7\text{H}_7^+$ ),

$$x = (y^2 - 1.42^2)^{1/2} = 1.69 \text{ \AA}$$

$$d_{\text{tube}} = d_{\text{cluster}} + 2x = 10 \text{ \AA} + 2 \cdot 1.69 \text{ \AA} = 13.4 \text{ \AA}$$

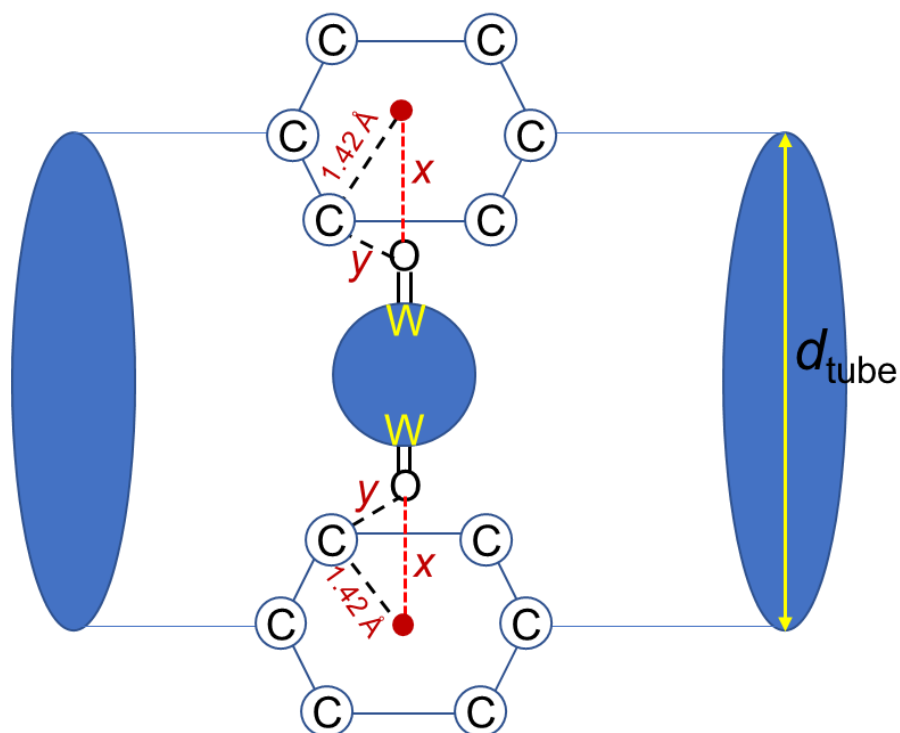


**Figure S9.** Model showing the estimation of the smallest SWCNT encapsulating a  $\{PW_{12}\}$  cluster.

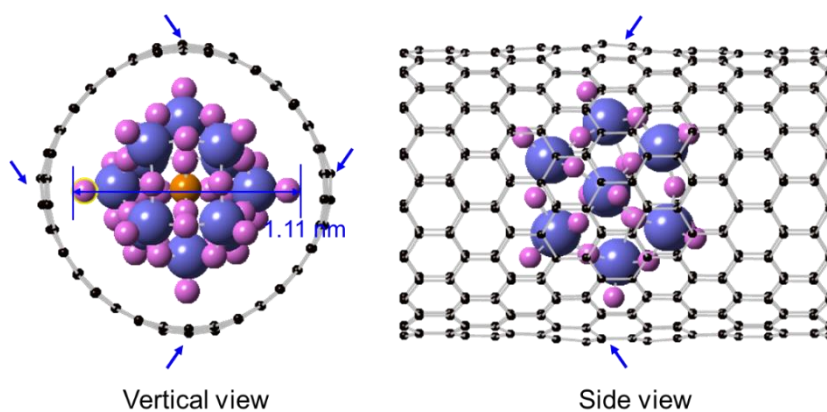


**Figure S10.** Vertical and side views of  $\{PW_{12}O_{40}\}@SWCNT$ s after DFT calculation. The distortion of SWCNT was marked by arrows.



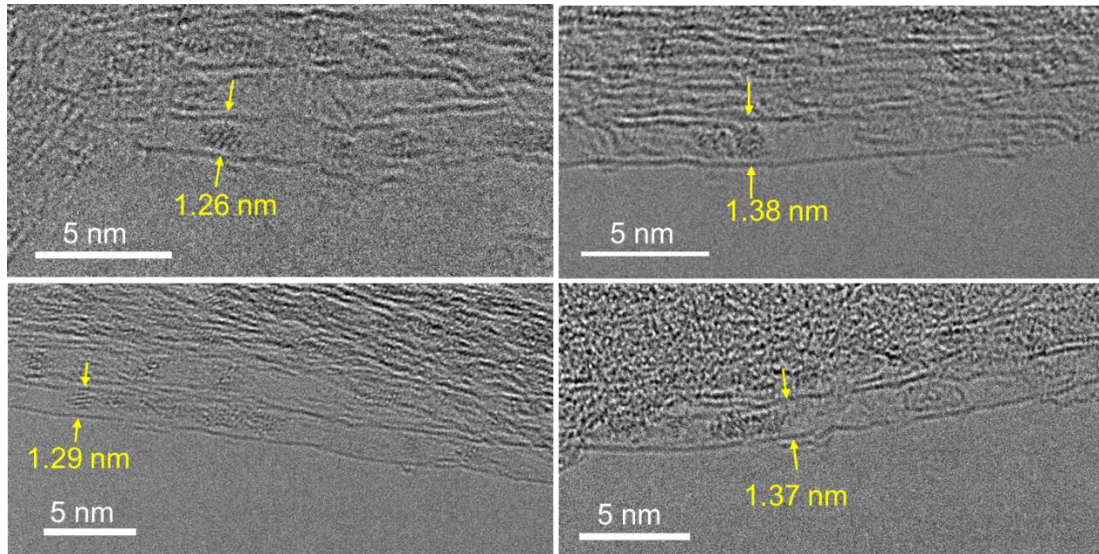


**Figure S11.** aberration-corrected TEM images of 1.26-1.38 nm SWCNTs encapsulating  $\{PW_{12}\}$  clusters.

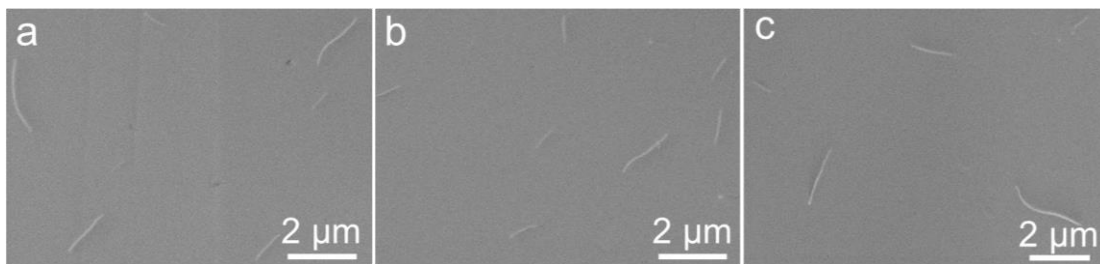


**Figure S12.** SEM images of individual dispersed  $\{PW_{12}O_{40}\}@Tuball-SWCNTs$  on Si/SiO<sub>2</sub> substrate. The sample was used to perform Raman at the single nanotube level.

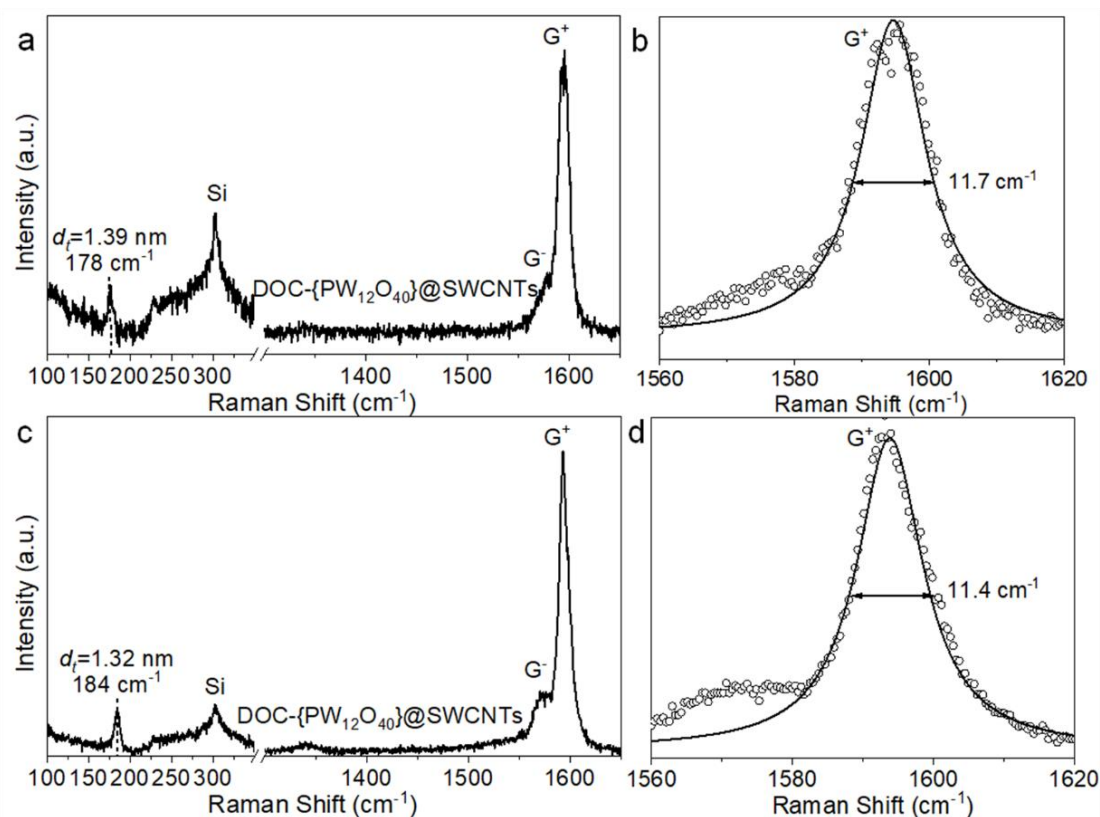


**Figure S13.** a–d, Raman spectra of individual  $\{PW_{12}O_{40}\}$ @Tuball-SWCNTs dispersed by DOC (a, c) and corresponding close-up view of  $G$  band region (b, d). Excitation: 532 nm.

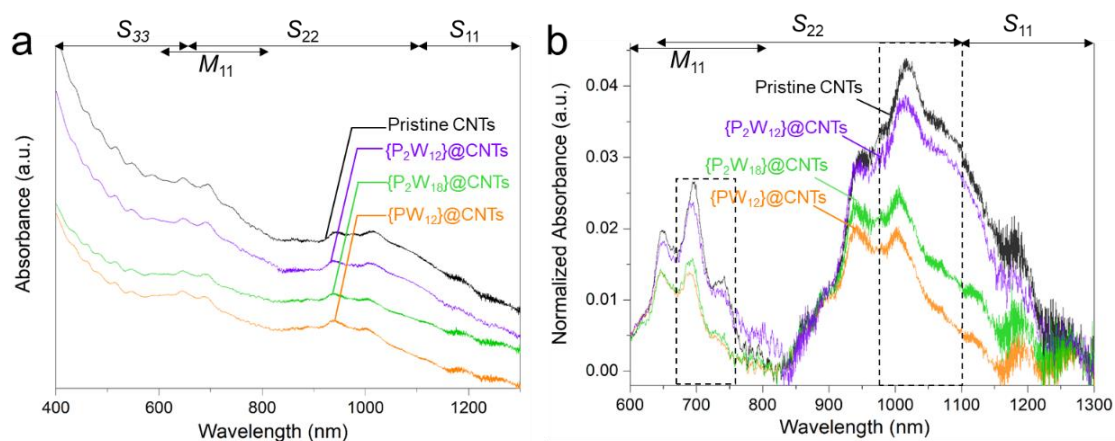


**Figure S14.** a, UV–Vis–NIR absorption spectra of DOC dispersed pristine SWCNTs and SWCNTs encapsulated with  $\{P_2W_{12}O_{48}\}$ ,  $\{P_2W_{18}O_{62}\}$ , and  $\{PW_{12}O_{40}\}$ . b, The baseline-subtracted absorption spectra in the  $S_{11}$ ,  $S_{22}$ , and  $M_{11}$  regions. The plot of  $\{PW_{12}O_{40}\}$ @CNTs and pristine CNTs in (a, b) were reproduced from Figure 3(a, b) in main text.

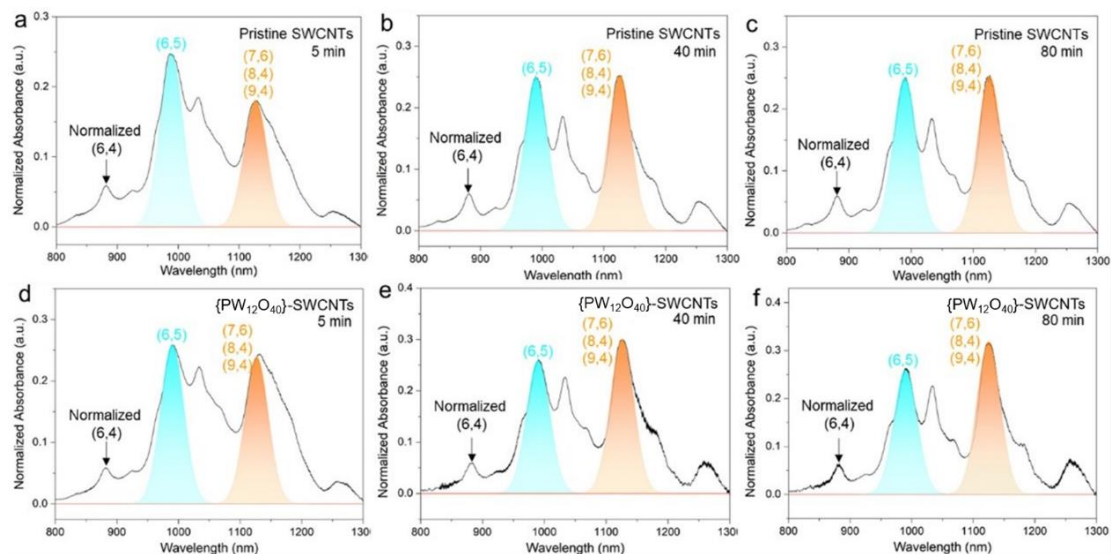


**Figure S15.** Absorption spectra (normalized at 880 nm) of sorted raw CoMo-SWCNTs and  $\{PW_{12}O_{40}\}$ -CoMo-SWCNTs with sonication time of 5, 40, and 80 min. The colored peaks were fitted with the same FWHM value of  $45\text{ cm}^{-1}$ .

**Table S1.** The relative peak area of sorted raw CoMo-SWCNTs and  $\{PW_{12}O_{40}\}$ -CoMo-SWCNTs with the chirality of (8,4)(9,4)(7,6) and (6,5) with different sonication time (5, 40, and 80 min).

Sample	DOC dispersed raw CoMo-SWCNTs		DOC dispersed $\{PW_{12}O_{40}\}$ -CoMo-SWCNTs	
	Absorption band	Absorption band	Absorption band	Absorption band
	989 nm	1126 nm	989 nm	1126 nm
	(6,5)	(8,4)(9,4)(7,6)	(6,5)	(8,4)(9,4)(7,6)
Fitted peak area $A_{(n,m)}$				
Sonication time	$A_{(6,5)}$	$A_{(8,4)(9,4)(7,6)}$	$A_{(6,5)}$	$A_{(8,4)(9,4)(7,6)}$
5 min	11.88	8.66	12.43	11.46
40 min	12.00	12.11	12.43	14.41
80 min	12.01	12.12	12.44	15.22

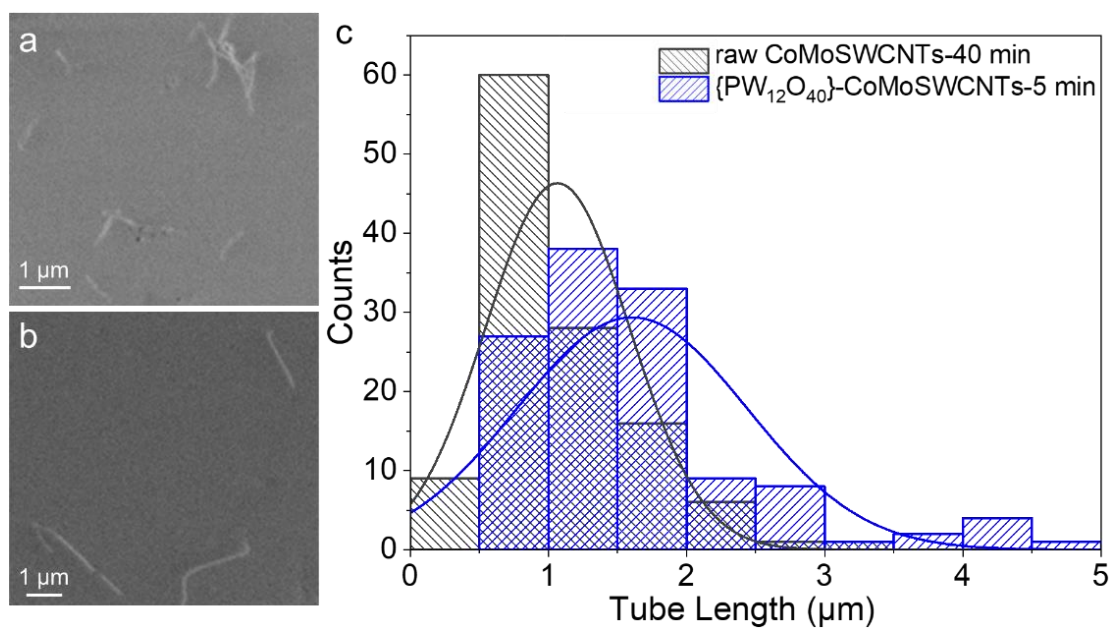


**Figure S16. a, b**, SEM images of {PW<sub>12</sub>O<sub>40</sub>}-CoMo-SWCNTs with 5 min sonication (a) and CoMo-SWCNTs with 40 min sonication (b) deposited on SiO<sub>2</sub>/Si substrate. c, The corresponding tube length distributions.

## Reference

1. X. Yang, T. Liu, R. Li, X. Yang, M. Lyu, L. Fang, L. Zhang, L. Zhang, A. Zhu, K. Wang, C. Qiu, Y. Z. Zhang, X. Wang, L.-M. Peng, F. Yang and Y. Li, *J. Am. Chem. Soc.*, 2021, **143**, 10120–10130.